

# Light fragment production at CERN Super Proton Synchrotron

Yu. B. Ivanov<sup>1,2,\*</sup> and A. A. Soldatov<sup>2,†</sup>

<sup>1</sup>*National Research Centre "Kurchatov Institute", 123182 Moscow, Russia*

<sup>2</sup>*National Research Nuclear University MEPhI (Moscow Engineering Physics Institute), Moscow 115409, Russia*

Recent data on the deuteron and  $^3\text{He}$  production in central Pb+Pb collisions at the CERN Super Proton Synchrotron (SPS) energies measured by the NA49 Collaboration are analyzed within the model of the three-fluid dynamics (3FD) complemented by the coalescence model for the light-fragment production. The simulations are performed with different equations of state—with and without deconfinement transition. It is found that scenarios with the deconfinement transition are preferable for reproduction rapidity distributions of deuterons and  $^3\text{He}$ , the corresponding results well agree with the experimental data. At the same time the calculated transverse-mass spectra of  $^3\text{He}$  at midrapidity do not that nice agree with the experimental data.

PACS numbers: 25.75.-q, 25.75.Nq, 24.10.Nz

Keywords: relativistic heavy-ion collisions, hydrodynamics, light fragments

## I. INTRODUCTION

Recently experimental data on light-fragment production in Pb+Pb collisions at SPS energies has been published by the NA49 Collaboration [1]. These data has been already theoretically analyzed in Refs. [1–3]. Traditionally the light-fragment data are interpreted within either the thermodynamical or coalescence models which in fact give results quantitatively close to each other [3]. The above-mentioned approaches are based on schematic fireball-like models which analyze total (or midrapidity) yields of light fragments. Nevertheless, the NA49 data include spectra in a wide range of rapidity and transverse momentum rather than only total yields. In the present study we would like to focus on the coalescence approach and to address the questions:

- (i) If the coalescence within 3D simulations is able to reproduce the rapidity and transverse-momentum spectra of light fragments rather than only their total (or midrapidity) multiplicities?
- (ii) If these spectra are sensitive to the equation of state (EoS) used in the simulations, in particular, to the deconfinement transition?

In the present paper the Pb+Pb collisions are simulated within the 3FD model [4] for several collision energies in the SPS energy range. The 3FD model is quite successful in reproduction of the major part of bulk observables in this range, among those the proton rapidity [5] and transverse-momentum distributions [6] are relevant to the present study. Light fragment formation (deuterons, tritons,  $^3\text{He}$  and  $^4\text{He}$ ) is taken into account in terms of the coalescence model, which is similar to that described in Appendix E of Ref. [7].

## II. COALESCENCE IN THE 3FD MODEL

Unlike the conventional hydrodynamics, where local instantaneous stopping of projectile and target matter is assumed, a specific feature of the 3FD description [4] is a finite stopping power resulting in a counterstreaming regime of leading baryon-rich matter. This generally nonequilibrium regime of the baryon-rich matter is modeled by two interpenetrating baryon-rich fluids initially associated with constituent nucleons of the projectile and target nuclei. In addition, newly produced particles, populating the midrapidity region, are associated with a fireball fluid. Each of these fluids is governed by conventional hydrodynamic equations coupled by friction terms in the right-hand sides of the Euler equations. These friction terms describe energy–momentum loss of the baryon-rich fluids. A part of this loss is transformed into thermal excitation of these fluids, while another part gives rise to particle production into the fireball fluid.

The physical input of the present 3FD calculations is described in Ref. [5]. The friction between fluids was fitted to reproduce the stopping power observed in proton rapidity distributions for each EoS, as it is described in Ref. [5] in detail. The simulations in [5, 6] were performed with different EoS's—a purely hadronic EoS [8] and two versions of the EoS involving the deconfinement transition [9], i.e. a first-order phase transition and a smooth crossover one. In the present study we use precisely the same parameters as those reported in Ref. [5].

We describe the fragment production within a coalescence model, in the spirit of refs. [10–12], similar to that it was done in Ref. [7]. We assume that  $N$  neutrons and  $Z$  protons, falling within a 6-dimensional phase volume  $(\frac{4}{3}\pi p_{NZ}^3)(\frac{4}{3}\pi r_{NZ}^3)$  at the freeze-out stage, form a  $(N, Z)$ -fragment. Here  $p_{NZ}$  and  $r_{NZ}$  are the parameters of the coalescence model, which are, in principle, different for different  $(N, Z)$ -fragments. For each impact parameter we calculate the distribution of observable  $(N, Z)$ -

\*e-mail: y.b.ivanov@yandex.ru

†e-mail: saa@ru.net

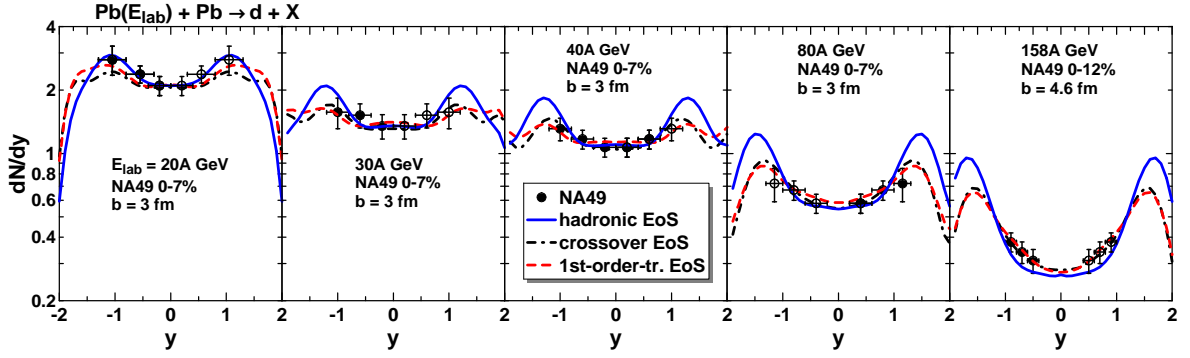


FIG. 1: Rapidity distributions of deuterons in central Pb+Pb collisions at various SPS energies ( $E_{\text{lab}}$ ) confronted to 3FD calculations with different EoS's. Experimental data are from the NA49 Collaboration [1]. The percentage indicates the fraction of the total reaction cross section, corresponding to experimental selection of events. The solid symbols show the measurements and the open symbols represent the data points reflected about mid-rapidity.

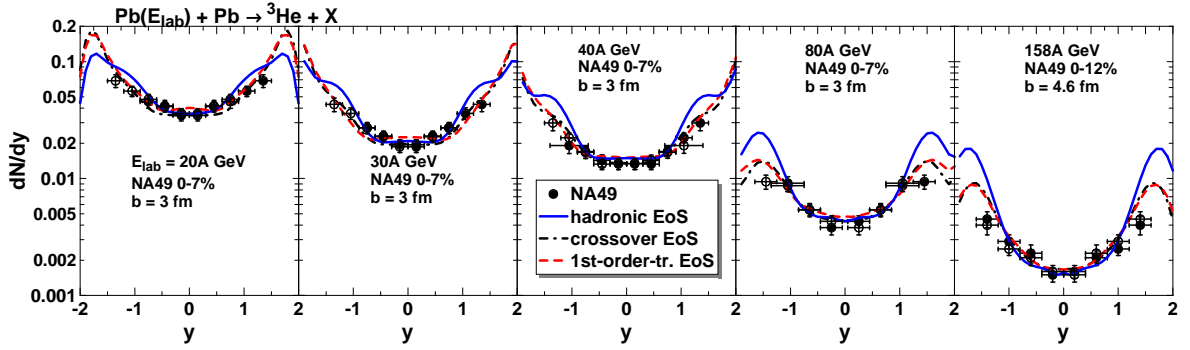


FIG. 2: The same as in Fig. 1 but for  ${}^3\text{He}$ .

fragments as follows (cf. [11, 13])

$$E_A \frac{d^3 \tilde{N}_{N,Z}}{d^3 P_A} = \frac{N_{\text{tot}}^N Z_{\text{tot}}^Z}{A_{\text{tot}}^A} A \frac{(\frac{4}{3} \pi p_{NZ}^3 / M_N)^{A-1}}{N! Z!} \times \left( \frac{V_{NZ}}{V} \right)^{A-1} \left( E \frac{d^3 \tilde{N}^{(N)}}{d^3 p} \right)^A. \quad (1)$$

Here  $N_{\text{tot}} = N_p + N_t$ ,  $Z_{\text{tot}} = Z_p + Z_t$  and  $A_{\text{tot}} = A_p + A_t$  are the total numbers of neutrons, protons and nucleons in the projectile-plus-target nuclei, respectively,  $A = N + Z$ ,  $E_A = AE$ ,  $\mathbf{P}_A = A\mathbf{p}$  and  $V_{NZ} = \frac{4}{3} \pi r_{NZ}^3$ .  $V = \bar{A}_{\text{tot}}/n_c$  is the total volume of the frozen-out system, where  $n_c$  is the freeze-out density and

$$\bar{A}_{\text{tot}} = \int d^3 p \frac{d^3 N^{(N)}}{d^3 p} \quad (2)$$

is the total number of primordial participant nucleons. Here we denote the distributions of observable (i.e. after the coalescence) nucleons and fragments by a tilde sign, in contrast to the primordial nucleon distribution. Unlike refs. [11, 13], we formulate the coalescence in terms of invariant distributions  $E d^3 N / d^3 p$  and also introduce the factor  $(V_{NZ}/V)$ , taking into account a vicinity in the coordinate space. This factor also provides a proper limit

at  $V \rightarrow \infty$ :  $E_A d^3 \tilde{N}_{N,Z} / d^3 P_A \sim V$ . Defining a new parameter

$$P_{NZ}^3 = \frac{4}{3} \pi p_{NZ}^3 V_{NZ} n_c \left( \frac{A}{N! Z!} \right)^{1/(A-1)}, \quad (3)$$

we can write down eq. (1) in a simpler form

$$E_A \frac{d^3 \tilde{N}_{N,Z}}{d^3 P_A} = \frac{N_{\text{tot}}^N Z_{\text{tot}}^Z}{A_{\text{tot}}^A} \left( \frac{P_{NZ}^3}{M_N \bar{A}_{\text{tot}}} \right)^{A-1} \left( E \frac{d^3 \tilde{N}^{(N)}}{d^3 p} \right)^A. \quad (4)$$

These equations for different  $N$  and  $Z$  form a set of equations, since the nucleon distribution in the r.h.s. is an observable distribution rather than a primordial one. To make this system closed, one should add a condition of the baryon number conservation

$$E \frac{d^3 N^{(N)}}{d^3 p} = E \frac{d^3 \tilde{N}^{(N)}}{d^3 p} + \sum_{N,Z (A>1)} A^3 E_A \frac{d^3 \tilde{N}_{N,Z}}{d^3 P_A}. \quad (5)$$

The  $P_{NZ}$  parameters are fitted to reproduce normalization of spectra of light fragments.

### III. RESULTS

Table I presents results of the fit of the  $P_{NZ}$  parameters to the NA49 data [1]. There is a clear trend of  $P_{NZ}$  reduction with collision energy rise. This can be associated with properties of the freeze-out procedure adopted in the 3FD model [14]. The freeze-out locally starts when the local energy density drops below some value (0.4 GeV/fm<sup>3</sup> in the present simulations). The thermal part of the energy density increases with the collision energy rise. Therefore, the compressional part drops, so does the freeze-out baryon density [ $n_c$ , see Eq. (3)]. This trend is less visible in the case of <sup>3</sup>He. Moreover, the  $P(^3\text{He})$  parameter stays constant at  $E_{\text{lab}} = 20, 30$  and  $40$  A·GeV. This is another representation (however, less spectacular) of the maximum in the  $N(^3\text{He})N(p)/N^2(d)$  ratio found in Ref. [2] and interpreted as a signature of a critical endpoint.

The above mentioned decrease of the freeze-out baryon density is illustrated in Table I. The displayed mean freeze-out baryon density is calculated within the crossover scenario for Pb+Pb collisions at impact parameters  $b = 2.4$  fm for  $E_{\text{lab}} = 20\text{A}-80\text{A}$  GeV and  $b = 4.6$  fm for  $E_{\text{lab}} = 158\text{A}$  GeV, which correspond the experimental centrality selection. In order to remove the  $n_c$  dependence from the  $P_{NZ}$  parameters, these parameters were reduced to the normal nuclear density ( $n_0 = 0.15$  fm<sup>-3</sup>):  $P_{NZ}(n_0/n_c)^{1/3}$ , cf. Eq. (3). As it is seen from Table I, these reduced parameters are constant in the considered energy range with the accuracy of  $\sim \pm 5\%$ , as it should be in the spirit of the used version of the coalescence model. Though the  $P(^3\text{He})(n_0/n_c)^{1/3}$  parameter manifests a trend of slight increase with the energy rise. The data on tritons were not analyzed because their experimental accuracy is much lower than that for deuterons and <sup>3</sup>He.

$E_{\text{lab}}$	[A·GeV]	20	30	40	80	158
$P(d)$	[MeV/c]	513	471	466	431	425
$P(^3\text{He})$	[MeV/c]	681	681	679	661	658
$n_c/n_0$		0.61	0.61	0.57	0.48	0.43
$P(d)(n_0/n_c)^{1/3}$	[MeV/c]	606	563	621	596	605
$P(^3\text{He})(n_0/n_c)^{1/3}$	[MeV/c]	805	804	818	845	874

TABLE I: Coalescence parameters, see Eq. (3), used in 3FD simulations of Pb+Pb collisions at various incident energies  $E_{\text{lab}}$ , the corresponding mean baryon densities ( $n_c$ ) at the freeze-out divided by normal nuclear density ( $n_0$ ) calculated within the crossover scenario, and the reduced parameters  $P_{NZ}(n_0/n_c)^{1/3}$ .

Results for the rapidity distributions of deuterons and <sup>3</sup>He in central Pb+Pb collisions at various SPS energies are presented in Figs. 1 and 2, respectively. As a rule, scenarios with deconfinement transition perfectly reproduce the NA49 data [1]. The hadronic scenario looks preferable only for deuterons at 20A GeV. We would like

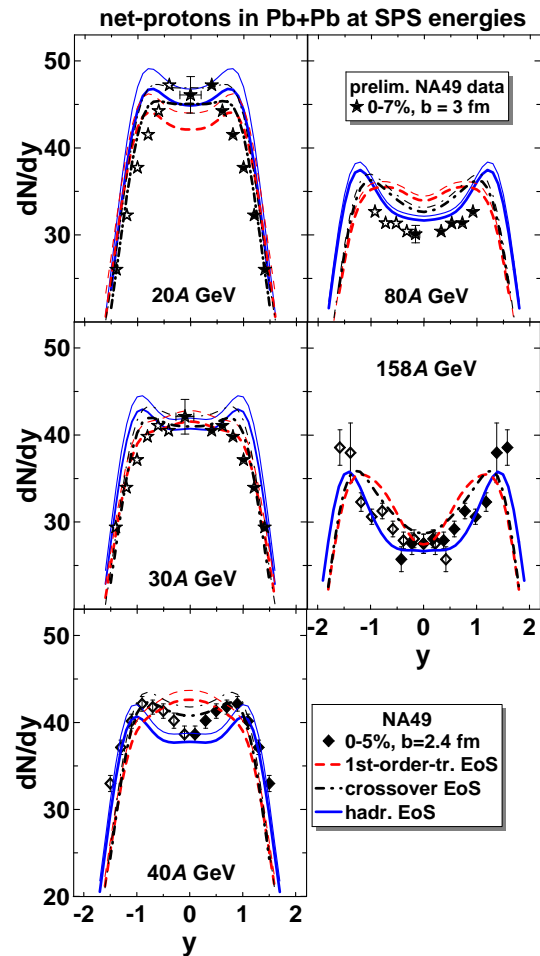


FIG. 3: Rapidity distributions of net-protons in central Pb+Pb collisions at SPS energies calculated within three considered scenarios. Thin lines display results without subtracting the contribution of light fragments, these were earlier reported in Ref. [5]. Bold lines present the results corrected by subtracting the contribution of light fragments. Experimental data are from the NA49 collaboration [16–20]. The percentage shows the fraction of the total reaction cross section, corresponding to experimental selection of events.

to remind that these results are achieved with only a single parameter for each distribution which determines the overall normalization of the spectrum. Correspondence between the fraction of the total reaction cross section related to a data set and a mean value of the impact parameter ( $b$  in Figs. 1 and 2) was read off from the paper [15].

Protons bound in light fragments should be subtracted from the calculated proton yield in order to compare the latter with observable proton data. At lower SPS energies this light-fragment correction is sizable. Rapidity distributions of net-protons in central Pb+Pb collisions at SPS energies calculated with and without this correction are presented in Fig. 3. The net-proton distributions without the light-fragment correction were earlier reported in Ref. [5]. The light-fragment correction is indeed notice-

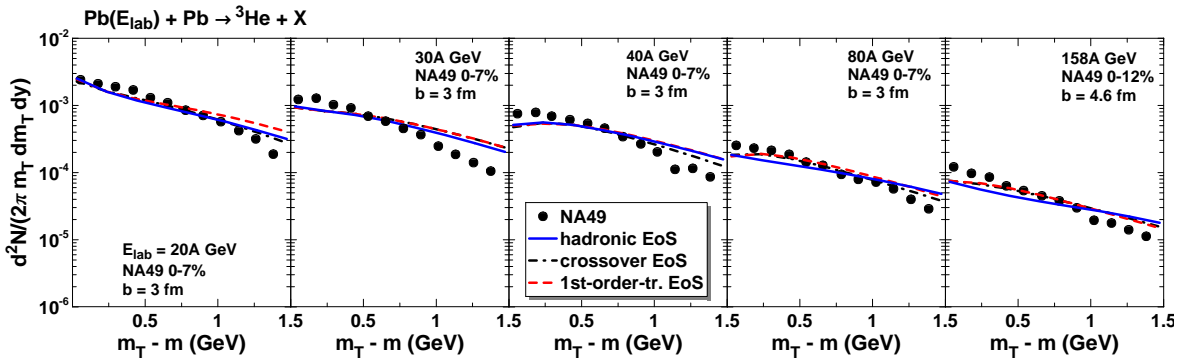


FIG. 4: Transverse-mass spectra of  ${}^3\text{He}$  at midrapidity in central Pb+Pb collisions at various SPS energies ( $E_{\text{lab}}$ ) confronted to 3FD calculations with different EoS's. Experimental data are from the NA49 Collaboration [1]. The percentage indicates the fraction of the total reaction cross section, corresponding to experimental selection of events.

able at 20A GeV and improves agreement of the crossover results with experimental data. Note however that the data at 20A GeV and 30A GeV still have preliminary status, and hence it is too early to draw any solid conclusions from comparison with them. The light-fragment correction at 158A GeV is practically negligible.

Figure 4 presents the comparison of transverse-mass spectra of  ${}^3\text{He}$  at midrapidity with experimental data from Ref. [1]. Here the agreement with the data is not that nice as that for the rapidity distributions. Moreover, different scenarios (with and without the deconfinement transition) fail approximately to the same extent. At the same time, within all considered scenarios the midrapidity transverse-mass spectra of protons are well reproduced in the low- $m_T$  range [6] which is relevant to the present light-fragment data. This discrepancy could however be expected in advance in view of  $p_T$  dependence of the coalescence coefficients deduced in Ref. [1].

#### IV. SUMMARY

Within the 3FD model complemented by the coalescence model at the freeze-out stage we have studied light-fragment production in Pb+Pb collisions at SPS energies and compared the obtained results with recently published data by the NA49 Collaboration [1]. The simulations were performed with different equations of state—a purely hadronic EoS [8] and two versions of the EoS involving the deconfinement transition [9], i.e. a first-order phase transition and a smooth crossover one.

It is found that scenarios with the deconfinement transition [9] are preferable for reproduction rapidity distributions of deuterons and  ${}^3\text{He}$  in the considered energy range, except for the case of deuterons at 20A GeV where

the hadronic scenario is slightly preferable. At the same time the transverse-mass spectra of  ${}^3\text{He}$  at midrapidity are not in that nice agreement with experimental data from Ref. [1]. Moreover, different scenarios (with and without the deconfinement transition) fail approximately to the same extent. This is in spite of good reproduction of the proton midrapidity transverse-mass spectra (within all considered scenarios) in the low- $m_T$  range [6] which is relevant to the present light-fragment data. If this is a signature of poor applicability of the coalescence mechanism to the light-fragment production or an indication of importance of an afterburner stage of the collision (i.e. the hadronic cascade after the freeze-out) is still an open question.

It would be instructive to compare the coalescence results with those of the thermodynamical approach to the light-fragment production also based on the 3FD simulations. This question can be answered within the framework of recently developed 3FD event generator complemented by the Ultra-relativistic Quantum Molecular Dynamics (UrQMD) for the afterburner stage—a Three-fluid Hydrodynamics-based Event Simulator Extended by UrQMD final State interactions (THESEUS) [21]—because the thermal fragment production has been already incorporated in it [22].

#### Acknowledgments

This work was carried out using high-performance computing resources of federal center for collective usage at NRC Kurchatov Institute, <http://computing.kiae.ru/>. This work was partially supported by the Academic Excellence Project of the NRNU MEPhI under contract No. 02.A03.21.0005.

[1] T. Anticic *et al.* [NA49 Collaboration], Phys. Rev. C **94**, no. 4, 044906 (2016) [arXiv:1606.04234 [nucl-ex]].

[2] K. J. Sun, L. W. Chen, C. M. Ko and Z. Xu, arXiv:1702.07620 [nucl-th].

- [3] S. Mrowczynski, arXiv:1607.02267 [nucl-th].
- [4] Yu. B. Ivanov, V. N. Russkikh, and V.D. Toneev, Phys. Rev. C **73**, 044904 (2006) [nucl-th/0503088].
- [5] Yu. B. Ivanov, Phys. Rev. C **87**, 064904 (2013) [arXiv:1302.5766 [nucl-th]].
- [6] Y. B. Ivanov, Phys. Rev. C **89**, no. 2, 024903 (2014) [arXiv:1311.0109 [nucl-th]].
- [7] V. N. Russkikh, Y. B. Ivanov, Y. E. Pokrovsky and P. A. Henning, Nucl. Phys. A **572**, 749 (1994).
- [8] V. M. Galitsky and I. N. Mishustin, Sov. J. Nucl. Phys. **29**, 181 (1979).
- [9] A. S. Khvorostukhin, V. V. Skokov, K. Redlich, and V. D. Toneev, Eur. Phys. J. **C48**, 531 (2006) [nucl-th/0605069].
- [10] H. Gutbrod et al., Phys. Rev. Lett. **37**, 667 (1976).
- [11] I. Gosset et al., Phys. Rev. **C16**, 629 (1977).
- [12] J. I. Kapusta, Phys. Rev. **C21**, 1301 (1980).
- [13] S. Das Gupta and A. Z. Mekjian, Phys. Rep. **72**, 131 (1981).
- [14] V. N. Russkikh and Yu. B. Ivanov, Phys. Rev. C **76**, 054907 (2007) [nucl-th/0611094]; Yu. B. Ivanov and V. N. Russkikh, Phys. Atom. Nucl. **72**, 1238 (2009) [arXiv:0810.2262 [nucl-th]].
- [15] C. Alt *et al.* [NA49 Collaboration], Phys. Rev. C **68**, 034903 (2003) [nucl-ex/0303001].
- [16] H. Appelshäuser *et al.* (NA49 Collab.), Phys. Rev. Lett. **82**, 2471 (1999).
- [17] T. Anticic *et al.* (NA49 Collab.), Phys. Rev. C **69**, 024902 (2004).
- [18] C. Alt *et al.* (NA49 Collab.), Phys. Rev. C **73**, 044910 (2006) [nucl-ex/0512033].
- [19] C. Blume (NA49 Collab.), J. Phys. **G34**, S951 (2007) [nucl-ex/0701042].
- [20] T. Anticic *et al.* [NA49 Collaboration], Phys. Rev. C **83**, 014901 (2011) [arXiv:1009.1747 [nucl-ex]].
- [21] P. Batyuk *et al.*, Phys. Rev. C **94**, 044917 (2016) [arXiv:1608.00965 [nucl-th]].
- [22] N.-U. Bastian *et al.*, Eur. Phys. J. A **52**, no. 8, 244 (2016) [arXiv:1608.02851 [nucl-th]].